IOP Conf. Series: Materials Science and Engineering **365** (2018) 042082 doi:10.1088/1757-899X/365/4/042082

# Bearing capacity of foundations base under combined alternating long-term static and cyclic loading

**Ilizar Mirsayapov and Danil Sabirzyanov**

Kazan State of Architecture and Engineering, Kazan, Russia

E-mail: mirsayapov1@mail.ru, danil198900@mail.ru

**Abstract**. Proposed a method for calculating the ground bases bearing capacity at combined alternating long-term static and cyclic loads. In graphical and analytical form, described the results of changes in the initial and transformed clay grounds deformation diagrams under combined alternating cyclic and long-term static loads, the ground strength and deformation properties.

## 1. Introduction

In the current design standards, the existing bearing capacity and deformations calculation methods are mainly designed for short-term static or cyclic loading with taking into account that the load data is constant for the entire period of the building or structure construction and operation. However, the accepted normative analytical calculations are not able to take into account the base of foundations deformation features under a successive alternation of long static and cyclic loads. Especially these issues are relevant for the foundations which folded from clay grounds with pronounced rheological properties.

In clay grounds, in combined loading cases, the stress-deformation state changes from the applied amounts of cyclic loading and the holding time under the long-term static load action, and also depends from the change in the ground strength and deformation properties at the previous loading blocks.

Proceeding from this, it becomes necessary to modernize the bearing capacity analytical calculation method with taking into account changes in the clay grounds deformation and strength properties in conditions of a triaxial stress state under combined alternating long-term static and cyclic loading.

The In design standards (SP 22.13330.2016), groundbase ultimate bearing capacity evaluation in the case of short-term static loading is carried out according to the following formula:

$$N_u = b' \cdot l' \cdot (N_\gamma \cdot \xi_\gamma \cdot b' \cdot \gamma_1 + N_q \cdot \xi_q \cdot \gamma_1' \cdot d + N_c \cdot \xi_c \cdot c_1) \quad (1)$$

where $N_\gamma, N_q, N_c$ = the ground dimensionless bearing capacity coefficients under the base of the foundation, depending on the ground internal friction angle $\varphi_i$;

$\xi_\gamma, \xi_q, \xi_c$ = coefficients, that depends from the ratio of length and the cross section width;

$l'$ and $b'$ = the foundation length and width, m;

$\gamma_1, \gamma_1'$ = the ground specific weight under the foundation bottom.

## 2. Experimental researches

As seen from 1, the limiting calculated ground resistance values and the ultimate load capacity depends from the internal friction angle and the ground specific cohesion.

For clay grounds with rheological properties, the internal friction angle $\varphi_1$ and specific cohesion $c_1$ are not constant values, but depends from the action time of a long-term static stress, amount of applied cyclic loading and from the action of the regime combined long-term static and cyclic stress.

In this connection, were carried out experimental and theoretical researches of clay grounds with disturbed structure under static, cyclic and combined long-term static and cyclic loading under triaxial compression conditions, with the following characteristics: $W$=23%; $W_p$=22.8 %; $W_L$=40.1 %; $\rho$=1.94 g/cm$^3$; $I_p$=17.3%; $I_L$=0.012.

Based on the experimental researches results, were obtained graphical and analytical dependences of changes in the strength and deformation characteristics of disturbed structure clay grounds during a short-term static, cyclic, long-term static and combined alternating cyclic and long-term static loads.

1.

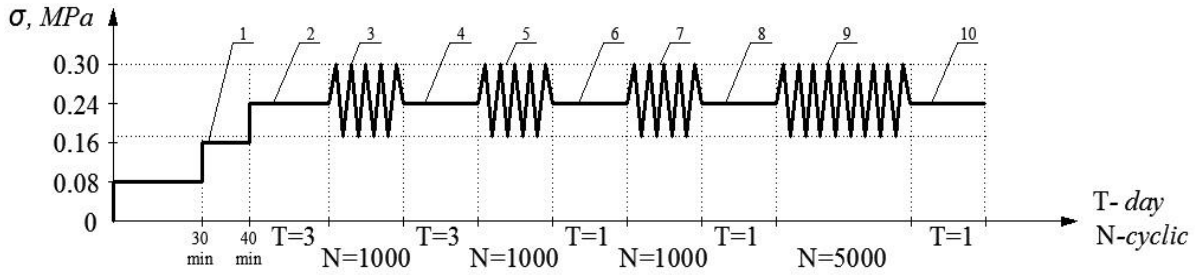


2.a)

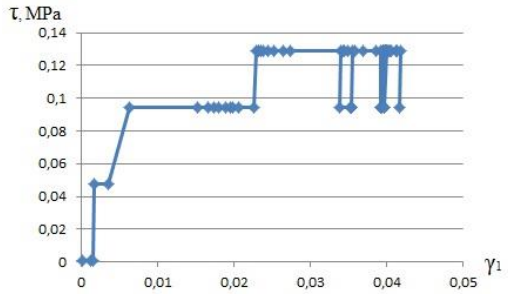


b)

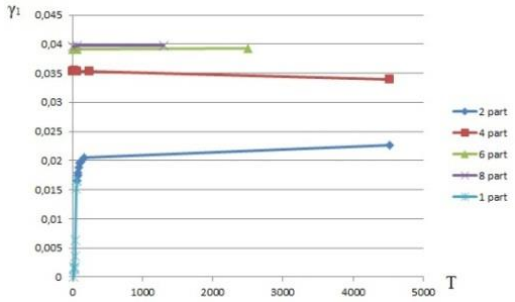


c)

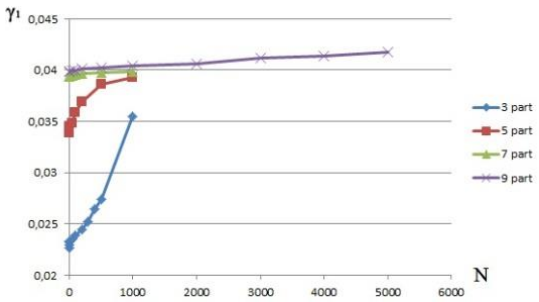


**Figure 1.** 1) The loading regime; 2) Dependency graphs under regime loading: a) shear stress from shear deformation; b) shear deformation from the time; c) shear deformation from the cycles;

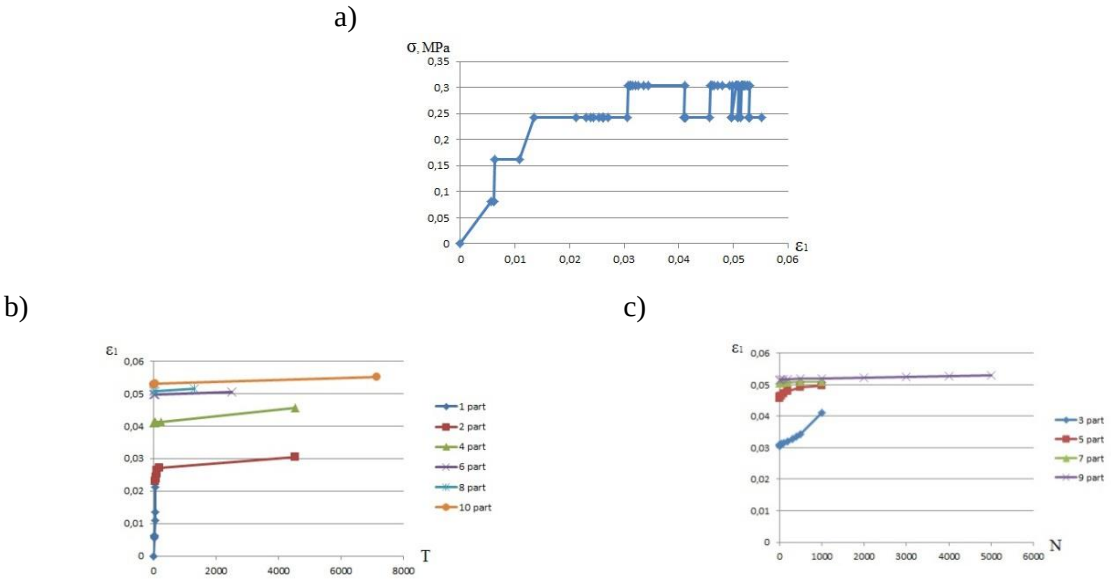


**Figure 2.** Dependency graphs under regime loading: a) vertical stress from vertical deformation; b) vertical deformation from time; c) vertical deformation from cycles

## 3. Analytical diagram of ground deformation under triaxial compression

Analyzing the clay grounds experimental researches results under combined alternating long-term static and cyclic loading (Fig. 1,2), it is evident that changes all clay grounds deformation and strength parameters. Therefore, as a mechanical state setting parameter of the ground under the regime loading, accepted the ground deformation analytical diagram in coordinates «$\sigma_1 - \varepsilon_1$», «$\tau_1 - \gamma_1$» for triaxial compression (where, $\sigma_1, \varepsilon_1$ vertical stresses and linear deformations, $\tau_1$, $\gamma_1$ vertical limiting shear stresses and shear deformations at triaxial compression).

Generalizing the experimental researches results, are constructed **initial diagrams** (state diagrams) of ground deformation at short-time triaxial static loading in coordinates $\sigma_1 - \varepsilon_1$ and $\tau_1 - \gamma_1$ (Fig. 3). The limiting point in coordinates ($\tau$) accepted value of the limiting shear stress $\tau_1 = \tau_{gr,u}$, and ($\sigma_1$) the value of the ground limiting resistance in a triaxial short-term static loading. The limiting point along the ordinate axis ($\gamma$) is the value of the shear deformation $\gamma_{u1} = 0{,}074$, and the value of the linear deformation ($\varepsilon$) is accepted as $\varepsilon_{u1} = 0{,}1$.

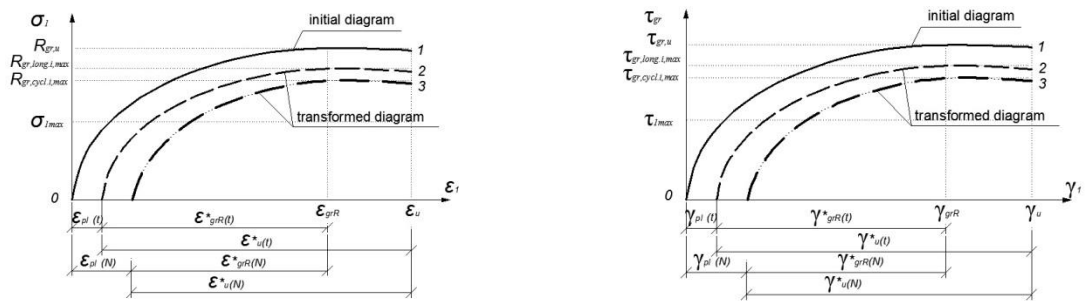


**Figure 3.** Graphs of changes in the ground deformation initial and transformed diagrams under loading: 1) short-term static; 2) long-term static

At modernizing the initial state diagram, are obtained equations that describe the clay ground deformation diagrams under triaxial long-term static loading. **Transformed diagrams** are accepted similarly to the initial state diagram based on the following positions (Figure 3):

- the maximum admissible values of the vertical shear and normal stresses, at the diagram top accepted shear and normal stresses in the ground, which is equal to the long-term resistance limit at a triaxial load $\tau_{gr,long}(t,\tau), R_{gr,long}(t,\tau)$, and deformations equal to the deformations at the top of ground state diagram under triaxial short-term static loading $\gamma_{gru,red} = \gamma_{gru}$, $\varepsilon_{gru,red} = \varepsilon_{gru}$;

- the maximum admissible values along the deformation axis defining the state diagrams limits, the shear creep deformation is equal to the limiting shear deformations with a triaxial short-term static loading $\gamma_{gr,red} = \gamma_{gr,R}$, and the vertical creep deformations equals the limiting deformations $\varepsilon_{gr,red} = \varepsilon_{gr,R}$ under the same loads, and the main dependences (2,3) calculate the stresses in ground;

- the diagrams origin are taken as displaced by an amount equal to the shear creep deformation $\gamma_{pl}(t)$ (4) and vertical deformations $\varepsilon_{pl}(t)$ (5) at the observed time moment - under long-term static loading

The equation of the maximum admissible values at the top diagram under a triaxial long-term static loading has the following form:

- vertical shear stress and loading time

$$\tau(t_1 t_0) = \tau_{gr,long} = -\alpha \ln(t) + \tau_{gr,u} \tag{2}$$

- vertical pressure and loading time

$$\sigma(t_1 t_0) = R_{gr,long} = -\alpha \ln(t) + R_{gr,u} \tag{3}$$

$\alpha$ = values obtained experimentally,

Deformations of the ground shear creep at the time moment with a long-term static loading accepted in the following equation:

$$\gamma_{pl}(t_1 t_0) = c_\infty(t_1\tau) \cdot \tau^{\max}(t_1 t_0) \cdot f(t_1 t_0) \cdot k_\gamma(t) \tag{4}$$

The ground creep deformations at the instant time moment under long-term static loading are determined by the formula:

$$\varepsilon_{pl}(t_1 t_0) = c_\infty(t_1\tau) \cdot \sigma(t_1 t_0) \cdot f(t_1 t_0) \cdot k_\varepsilon(t) \tag{5}$$

where $f(t_1 t_0) = 1 - e^{-\gamma(t-t_0)}$ = is the creep deformation growth function;

$\gamma$ = ground creep parameter;

$k_\varepsilon(t), k_\gamma(t)$ - coefficient that takes into account the nonlinear creep of ground deformation;

$k_\gamma(t)$ = 1.8, $k_\varepsilon(t)$ =1.6 at the first block of static loading from 1 to 3 days (up to cyclic loading);

$k_\gamma(t)$ = 1.65, $k_\varepsilon(t)$ =1.55 at subsequent blocks of long-term static loading;

$c_\infty(t_1\tau) = \dfrac{\gamma_{pl}(t_1\tau)}{\tau_{gr,u}(t_1\tau)}$, $c_\infty(t_1\tau) = \dfrac{\varepsilon_{pl}(t_1\tau)}{R_{gr,u}(t_1\tau)}$, = the limiting measure of ground creep at time moment t;

In the same way, by modernizing the initial state diagram, are obtained equations that describe the clay ground deformation diagrams under triaxial cyclic loading. **Transformed diagrams** are accepted similarly to the initial state diagram based on the following positions (Fig. 3):

- the maximum admissible values of the vertical shear and normal stresses, at the top of the diagram are accepted the shear and normal stresses in the ground, which equals to the limit of the

long-term resistance under triaxial load $\tau_{gr,long}(t,\tau), R_{gr,long}(t,\tau)$, and deformations equal to the deformations at the top of the ground state diagram under triaxial cyclic loading $\gamma_{gru,red} = \gamma_{gru}$, $\varepsilon_{gru,red} = \varepsilon_{gru}$;

- the maximum admissible values along the deformation axis defining the limits of the state diagrams, the shear creep deformations is equal to the limiting shear deformations under triaxial cyclic loading $\gamma_{gr,red} = \gamma_{gr,R}$, the vertical creep deformations equals the limiting deformations $\varepsilon_{gr,red} = \varepsilon_{gr,R}$ under the same loads, and by the main dependencies (6,7) calculate stresses in the ground;

- the diagrams origins are taken as displaced to amount, equal to the deformation of shear vibro-creep $\gamma_{pl}(N)$ (8) and vertical vibro-creep deformations $\varepsilon_{pl}(N)$ (9) in the observed loading cycle: - under cyclic loading.

The equation of the maximum admissible values at the state diagram top under triaxial cyclic loading has the following form:

- vertical shear stress and number of loading cycles

$$\tau(t_1\tau) = \tau_{gr,cycl}(N) = \tau_{gr,u} \cdot e^{-\beta N} \tag{6}$$

- vertical pressure and number of loading cycles

$$\sigma(t_1\tau) = R_{gr,cycl}(N) = R_{gr,u} \cdot e^{-\beta N} \tag{7}$$

β = values obtained experimentally;
N = the number of cyclic loads.

The ground shear creep deformations in the observed cycle at cyclic loading accepted the following form of the equation:

$$\gamma_{pl}(N) = \frac{c_\infty(t_1\tau) \cdot \tau^{\max}(t_1\tau) \cdot f(N) \cdot k_\gamma(N) \cdot \rho}{k_\rho} \tag{8}$$

The ground creep deformations in the observed cycle under cyclic loading are determined by the formula:

$$\varepsilon_{pl}(N) = \frac{c_\infty(t_1\tau) \cdot \sigma^{\max}(t_1\tau) \cdot f(N) \cdot k_\varepsilon(N) \cdot \rho}{k_\rho} \tag{9}$$

where $f(N) = 1 - e^{-\gamma(N_i - N_{i-1})}$ = the growth function of shear creep deformation;

$\gamma$ = ground shear creep parameter under cyclic loading;

$k_\varepsilon(N), k_\gamma(N)$ = coefficient, which depends from nonlinear ground creep deformation;

$k_\gamma(N)$ = 1.8, $k_\varepsilon(N)$ =1.37 at cyclic loading up to 1000 cycles;

$k_\gamma(N)$ = 1.65, $k_\varepsilon(N)$ =1.25 at cyclic loading after 1000 cycles;

$\rho$ = cycle asymmetry of vertical ground stresses;

$k_\rho$ = coefficient depending from $\rho$;

$c_\infty(t_1\tau) = \frac{\gamma_{pl}(t_1\tau)}{\tau_{gr,u}(t_1\tau)}$, $c_\infty(t_1\tau) = \frac{\varepsilon_{pl}(t_1\tau)}{R_{gr,u}(t_1\tau)}$ = the ground creep ultimate measure;

For the analytical description of the ground deformation diagrams (states), under combined alternating cyclic and long-term static loads, the dependences (2-9) are transformed for triaxial cyclic and long-term static loading (Fig. 4). At describing the ground creep deformation under combined loading, should be taken into account the vertical pressure influence ( $\sigma_1$ ) of the previous block to the strength, the deformation modulus, the shear modulus and the relative vertical deformations at the diagram top under subsequent loading after switching to another mode.

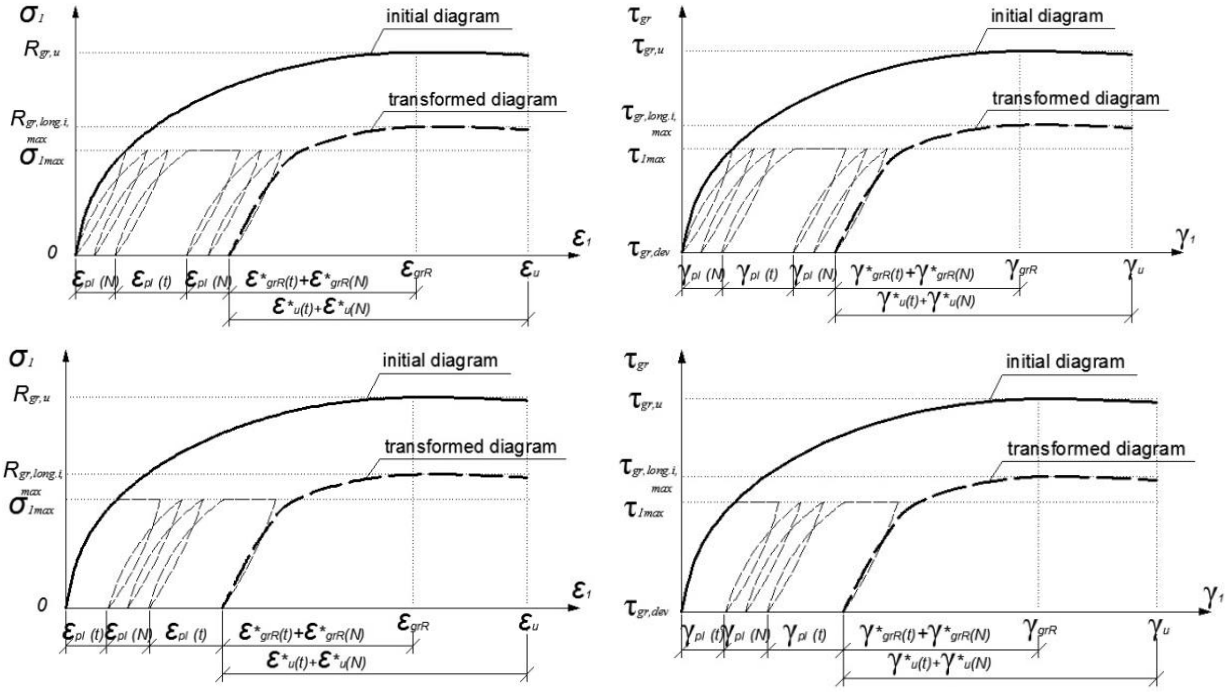


**Figure 4.** Change graphs in the initial and transformed diagrams of the ground deformation at long-term static and cyclic loading combination

In each block, the change in the deformation diagrams described by the same formulas as for a long-term static or cyclic loading, but suitable for each block $\sigma_{1i}, \tau_{1i}, N_i$ or $T_i$, on condition of change the strength and deformation strength parameters and deformability in the past load blocks.

In each new block, in depending on the type of loading, takes place the ground state diagram subsequent transformation, while the initial diagram for each block of them accepted as a transformed diagram at the end of the previous block.

Based on the obtained experimental and theoretical studies, on the graph 5 shows the changes in the limiting shear stress for a triaxial short-term static, long-term static, cyclic and at combined alternating long-term static and cyclic loads. It can be seen from the graphs that the limiting shear stress of clay samples under combined loading differs significantly from the limiting shear stresses for a long-term static and cyclic loading.

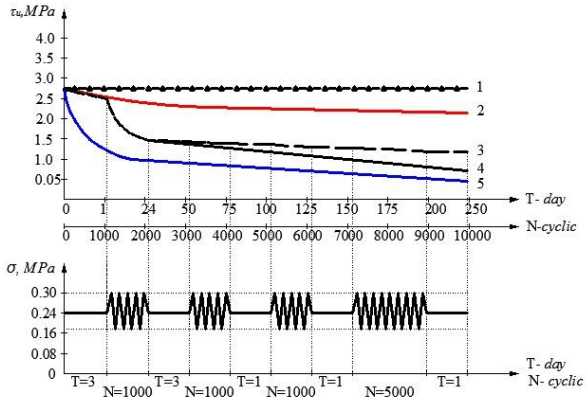


**Figure 5.** Change graph of the limiting shear stress at clay ground triaxial compression with a lateral pressure 0.08 MPa
1 - at short-term static loading; 2 - at long-term static loading; 3 - at combined long-term static and cyclic loading, taking into account the ground hardening; 4 - at combined long-term static and cyclic loading without taking into account ground hardening; 5 - at cyclic loading.

## 4. Theoretical researches

Further, by determining analytically the ultimate shear stress and the shear creep deformation of clay grounds under cyclic, long-term static and combined loading, the strength condition is taken according to the Coulomb-Mora law:

$$\tau_{ult}(N,T) = \sigma_1(N,T) \cdot tg\varphi(N,T) + c(N,T,\tau) \qquad (10)$$

where $\varphi(N,T), c(N,T,\tau)$ = clay ground strength characteristics with combined long-term static and cyclic loading (internal friction angle and specific cohesion);
$\sigma(N,T)$ = the normal maximum vertical stress.

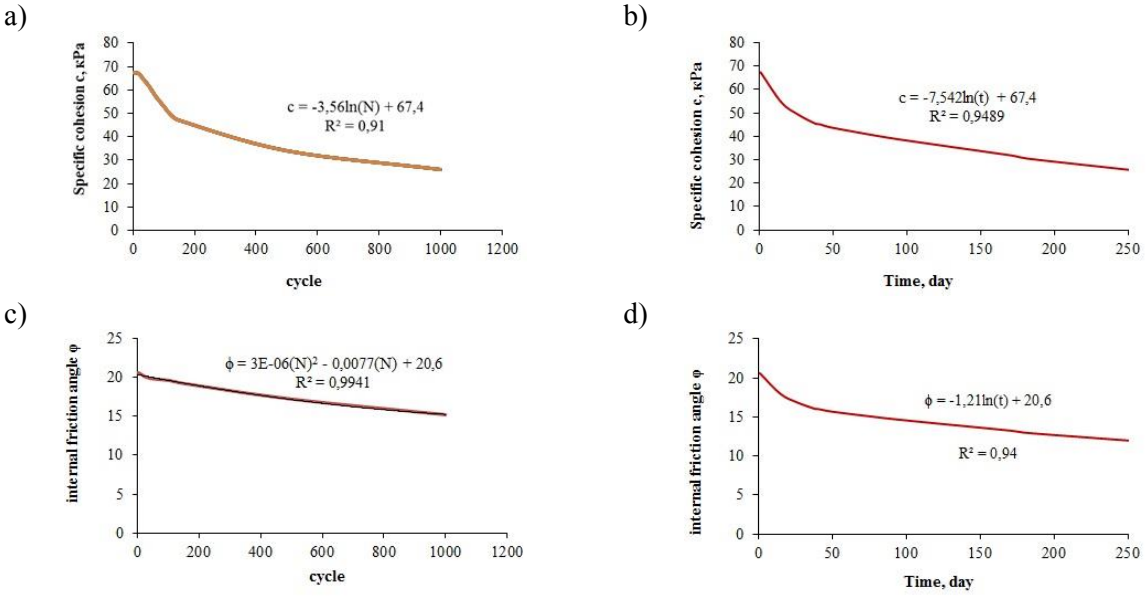


**Figure 6.** Clay ground strength characteristics:
- specific cohesion: a) at triaxial cyclic loading; b) at long-term static loading;
- internal friction angle: c) at triaxial cyclic loading; d) at long-term static loading

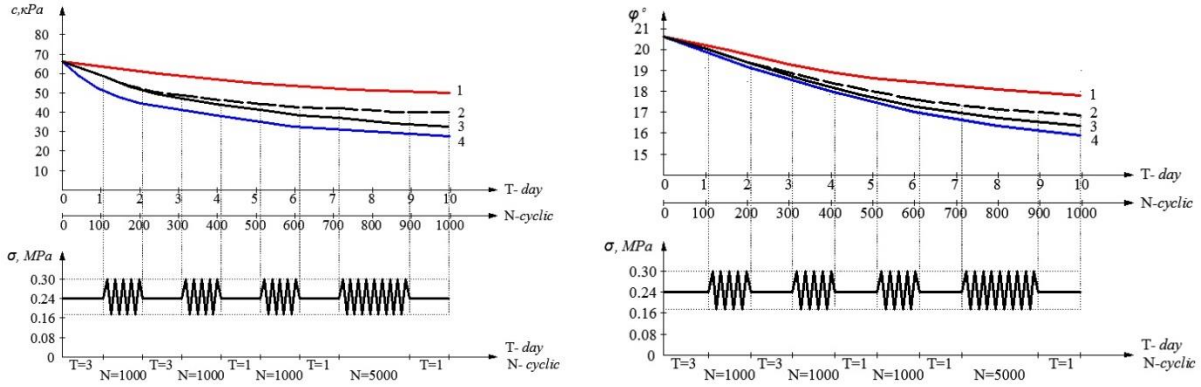


**Figure 7.** Clay ground changing in strength characteristics under a triaxial loading: a) specific cohesion; b) internal friction angle;
1) at long-term static loading; 2) at combined alternating long-term static and cyclic loading, taking into account ground hardening; 3) at combined alternating long-term static and cyclic loading without taking into account ground hardening; 4) at cyclic loading

In figures 6, 7 shows the changes in the clay ground strength characteristics under cyclic, long-term static and combined loads. It can be seen from the graphs that the decrease in strength parameters occurs mainly due to decrease of the specific cohesion $c$, while the internal friction angle $\varphi$ decreases insignificantly.

Based on the results of experimental studies (Fig. 7), the specific cohesion at the combined alternating cyclic and long-term static loads without taking into account the grounds hardening are presented in the following form:

$$c(N,T,\tau) = c_0 - \sum_{i=1}^{n} \Delta c(N) \pm \sum_{j=1}^{n} \Delta c(T) \tag{11}$$

where $c_0$ = the ground initial specific cohesion, corresponding to short-term static loading;

$c(N)$ = the ground specific cohesion under cyclic loading;

$c(T)$ = the ground specific cohesion under long-term static loading;

The ground specific cohesion in the considered cycle under under cyclic loading is determined by the formula:

$$\Delta c(N) = K_{\varepsilon}(N)\Delta\varepsilon^{p}(N) + K_{\gamma}(N)\Delta\gamma^{p}(N) \tag{12}$$

The ground specific cohesion at the time moment under a long-term loading is determined by the formula:

$$\Delta c(T) = K_{\varepsilon}(T)\Delta\varepsilon^{p}(T) + K_{\gamma}(T)\Delta\gamma^{p}(T) \tag{13}$$

where $K_{\varepsilon} = \Delta c / \Delta\varepsilon$ and $K_{\gamma} = \Delta c / \Delta\gamma$ - are parameters for the interrelation between $\Delta c$ and $\Delta\varepsilon, \Delta\gamma$, determined from the experiment;

For the calculation $K_{\gamma}$, we use the transformed grounds state diagrams made for regime loading, where it is seen how at the ground shear creep changes, the limiting shear stress is reduced. By the same principle, we find by constructing a transformed diagram between the vertical stress and the creep deformation.

Further, consider the process of clay ground hardening with combined alternating cyclic and long-term static loads. In clay grounds, depending on the load regime, value and duration, appear two compensating each other processes: hardening, which occurs due to the self-healing of cracks and the particles rearrangement, as well as the softening caused by the cracks development and the particles reorientation [Mirsayapov & Koroleva 2016, Mirsayapov & Koroleva 2017].

The results of experimental researches confirmed that, at combined alternating static and cyclic loading, the ground hardening increased from 5% to 20% due to the water-colloidal and structural connections restoration (Figs. 5 and 8).

Based on the foregoing, by processing the experimental data, was built a clay ground hardening coefficient change graph for a combined alternating static and cyclic loading (Fig. 8).

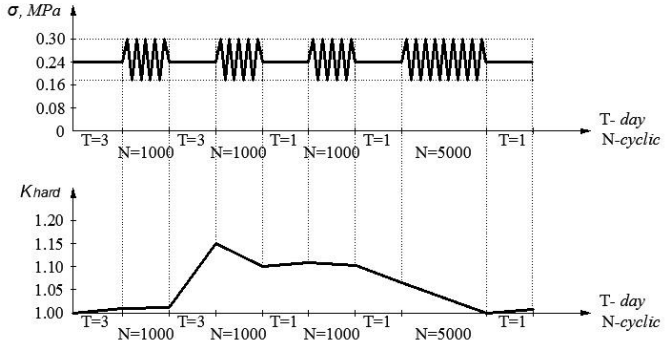


**Figure 8.** Change graph in the clay ground hardening coefficient under combined loading

Taking into account the hardening of clay ground, at combined alternating cyclic and long-term static loads, the change in ground specific cohesion in a certain loading interval is determined by the following formula:

$$\Delta c(N,T,\tau) = (\sum_{i=1}^{n}(K_{\varepsilon}(N,T)\cdot\sum_{j=1}^{n}(\frac{c_{\infty}(t_1\tau)\cdot\sigma^{\max}(t_1\tau)\cdot f(N)\cdot k(N)\cdot\rho}{k_{\rho}}+$$
$$+c_{\infty}(t_1\tau)\cdot\sigma^{\max}(t_1t_0)\cdot f(t_1t_0)\cdot k(t))+$$
$$+\sum_{k=1}^{n}(K_{\gamma}(N,T)\cdot\sum_{m=1}^{n}(\frac{c_{\infty}(t_1\tau)\cdot\tau^{\max}(t_1\tau)\cdot f(N)\cdot k(N)\cdot\rho}{k_{\rho}}+ \quad (14)$$
$$+c_{\infty}(t_1\tau)\cdot\tau^{\max}(t_1t_0)\cdot f(t_1t_0)\cdot k(t)))\cdot\frac{1}{k_{hard}}$$

where $K_{hard}(N,T)$ - the ground hardening coefficient under combined loading, determined from the graph (Fig. 7).

Then the ground specific cohesion under the combined long-term static and alternating cyclic loading are determined by the formula:

$$c(N,T,\tau) = c_0 - \Delta c(N,T,\tau) \quad (15)$$

Starting from formula (10) by using transformed clay ground deformation diagram (Fig. 4) at alternating regime long-term static and cyclic loading, knowing the specific cohesion at such loadings, changes in the ground internal friction angle is determined from the following equation:

$$\varphi(N,T,\tau) = arctg\left(\frac{\tau_{ult}(N,T) - c(N,T,\tau)}{\sigma_1(N,T)}\right) \quad (16)$$

By determining analytically the strength characteristics $\varphi(N,T,\tau)$ and $c(N,T,\tau)$ for the combined alternating cyclic and long-term static loads, the ultimate bearing capacity equation of the base is written as follows:

$$N_u = b' \cdot l' \cdot (N_\gamma \cdot \xi_\gamma \cdot b' \cdot \gamma_1 + N_q \cdot \xi_q \cdot \gamma_1' \cdot d + N_c \cdot \xi_c \times$$
$$\times (c_0 - (\sum_{i=1}^{n} (K_\varepsilon(N,T) \cdot \sum_{j=1}^{n} (\frac{c_\infty(t_1\tau) \cdot \sigma^{\max}(t_1\tau) \cdot f(N) \cdot k(N) \cdot \rho}{k_\rho} +$$
$$+ c_\infty(t_1\tau) \cdot \sigma^{\max}(t_1 t_0) \cdot f(t_1 t_0) \cdot k(t)) + \quad (17)$$
$$+ \sum_{k=1}^{n} (K_\gamma(N,T) \cdot \sum_{m=1}^{n} (\frac{c_\infty(t_1\tau) \cdot \tau^{\max}(t_1\tau) \cdot f(N) \cdot k(N) \cdot \rho}{k_\rho} +$$
$$+ c_\infty(t_1\tau) \cdot \tau^{\max}(t_1 t_0) \cdot f(t_1 t_0) \cdot k(t))) \cdot \frac{1}{k_{ynp}})$$

The ground bearing capacity function under the regime loading takes the form:

$$N_\gamma = \left(N_q - 1\right)\left(0{,}29 + 0{,}47 arctg\left(\frac{\tau_{ult}(N,T) - c(N,T,\tau)}{\sigma_1(N,T)}\right)\right);$$
$$N_q = tg^2\left(45^0 + \frac{\varphi_1}{2}\right) \cdot e^{\pi arctg\left(\frac{\tau_{ult}(N,T) - c(N,T,\tau)}{\sigma_1(N,T)}\right)}; \quad (18)$$
$$N_c = \frac{N_q - 1}{arctg\left(\frac{\tau_{ult}(N,T) - c(N,T,\tau)}{\sigma_1(N,T)}\right)}$$

For the approbation, the obtained ultimate bearing capacity equation of the base, were carried out clay ground tray tests with disturbed structure and the same characteristics as for triaxial tests.

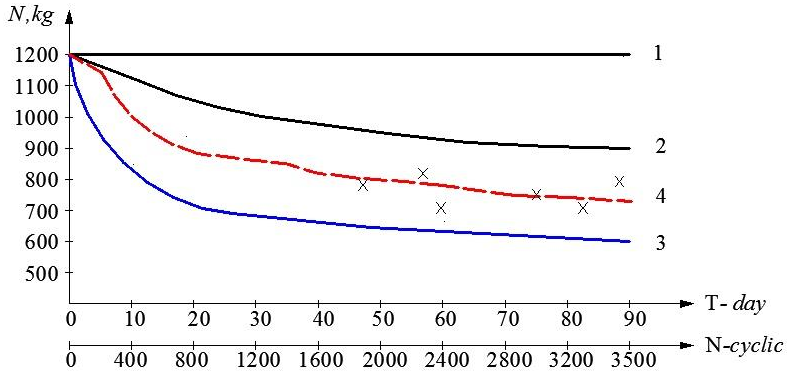


**Figure 9.** Comparison of the plate foundation ultimate bearing capacity at combined alternating static and cyclic loads
Change graphs ultimate bearing capacity at: 1) short-term static loading; 2) long-term static loading; 3) cyclic loading; 4) the proposed method (17)
x - experimental values under regime loading with considering the ground hardening;

From the graph 9, observed a good convergence between the developed ultimate bearing capacity calculation value of the base and experimental data.

## 5. Conclusion

Has been developed the ground base ultimate bearing capacity equation for combined alternating static and cyclic loads, which take into account the simultaneous change in the ground rheological and strength characteristics, the hardening process, and loading regimes.

The obtained equations adequately describe processes occurring in the ground under regime loading, which is confirmed by good agreement of the experimental data with the proposed equation.

## References

[1] Mirsayapov I T, Koroleva I V. (2011). Bearing capacity of foundations and rainfall with prolonged loading. *Integration, partnership and innovation in building science and education: the International Collection of papers. Scien. Conf. 2 t. Vol.2*, 342-347.

[2] Mirsayapov I T, Koroleva I V. (2009). Research strength and deformability of clay soils with prolonged triaxial compression. *Proceedings of the Kazan State Architectural University. No 2 (12),* 167-172.

[3] Mirsayapov I T, Koroleva I V, Sabizyanov D D. (2013). Strength and deformation of clayey soils under triaxial modal alternating static and cyclic loading. *Geotechnics Belarus: Science and Practice,* 297-304.

[4] Mirsayapov I T, Koroleva I V, Sabizyanov D D. (2014). Warp clay soils combined with the regime and the long-term cyclic loading. *Perspective directions of development of the theory and practice of rheology and soil mechanics. Proceedings of the XIV International Symposium on rheology*, 130-135.

[5] Mirsayapov I T , Koroleva I V. (2016). The strength and deformability of clay soils under the regime spatial stress state in view of cracking. *Grounds, foundations and soil mechanics*, *No 1*, 16-23.

[6] Mirsayapov I T, Koroleva I V, Sabirzyanov D D. (2016). Calculation model of the basement basement sediment under regime static-cyclic loading. *Proceedings of the Kazan State Architectural University. No 1 (35),* 102-110.

[7] Mirsayapov I T, Koroleva I V (2017) Influence of the hardening process on the strength of clayey soil under regime triaxial loading. *Proceedings of the Kazan State Architectural University. No 1 (39),* 145-152.

[8] Mirsayapov I T, Koroleva I V, Prediction of deformations of foundation beds with a consideration of long-term nonlinear soil deformation. *Soil Mechanics and Foundation Engineering. 2011. V. 48. No 4.* 148-157.